Laboratory evaluation of a gasifier particle sampling system using model compounds of different particle morphology

Nilsson, Patrik; Malik, Azhar; Pagels, Joakim; Lindskog, Magnus; Rissler, Jenny; Gudmundsson, Anders; Bohgard, Mats; Sanati, Mehri

Published in:
Biomass Conversion & Biorefinery

DOI:
10.1007/s13399-011-0010-6

2011

Laboratory evaluation of a gasifier particle sampling system using model compounds of different particle morphology

P. T. Nilsson*, A. Malik, J. Pagels, M. Lindskog, , J. Rissler, A. Gudmundsson, M. Bohgard and M. Sanati

Division of Ergonomics and Aerosol Technology, Lund University, P.O. Box 118, SE-22100, Lund, Sweden

*To whom the correspondence should be addressed. Email: Patrik.Nilsson@design.lth.se
Telephone: +46-46 222 3284, Fax: +46-46 222 4431

Abstract

The objective of this work was to design and evaluate an experimental setup to be used for field studies of particle formation in biomass gasification processes. The setup includes a high temperature dilution probe and a denuder to separate solid particles from condensable volatile material. The efficiency of the setup to remove volatile material from the sampled stream and the influence from condensation on particles with different morphologies is presented. In order to study the sampling setup model aerosols were created with a nebulizer, to produce compact and solid KCl particles, and a diffusion flame burner to produce agglomerated and irregular soot particles. The nebulizer and soot generator was followed by an evaporation-condensation section where volatile material, di-octyl-sebacete (DOS), was added to the system as a tar model compound. The model aerosol particles were heated to 200 ºC to create a system containing both solid particles and volatile organic material in gas phase. The heated aerosol particles were sampled and diluted at the same temperature with the dilution probe. Downstream the probe the DOS was captured by the denuder. This was achieved by slowly decrease the temperature of the diluted sample towards ambient level in the denuder. Thereby the supersaturation of organic vapors was reduced which decreased the probability for tar condensation and nucleation of new particles. Both the generation system and the sampling technique gave reproducible results. A DOS collection efficiency of >99% was achieved if the denuder inlet concentration was diluted to less than 1-6 mg/m^3 depending on the denuder flow rate. Concentrations higher than that lead to significant impact on the resulting KCl size distribution. The choice of model compounds was done to study the effect from the particle morphology on the achieved particle characteristics after the sampling setup. When similar amounts of volatile material condensed on soot agglomerates and compact particles, a substantially smaller growth in mobility diameter was found for soot compared to compact KCl.

Keywords: High temperature particle sampling, gasification, biomass, denuder, model aerosol, tar, particle morphology, APM, effective density, soot

1. Introduction

Thermochemical conversion of biomass consists of combustion and gasification. Combustion takes place in an environment rich in oxygen, while gasification processes occur in reducing environment. Consequently, the mass concentration of fly ash from combustion processes is dominated by inorganic compounds [1-3], while carbonaceous compounds dominate the particulate matter obtained from gasification [4-9]. Formation of fine

particles in these processes is troublesome because it initiates corrosion and fouling on interior surfaces, such as in the furnace and the heat exchangers. Formation of fine particles may also lead to catalytic deactivation in downstream processing for production of biofuels and chemicals [10-12].

Removal of gaseous impurities such as ammonia and sulfur can be performed by chemical methods whereas removal of fine particulates is traditionally performed using mechanical purification [13-17]. To ensure performance of the subsequent upgrading processes the produced gas usually has to be cooled down to moderate temperatures in order to convert a major portion of the impurities from the gas to particulate phase, and to be able to effectively utilize purification devices that operate at a moderate temperature range. The cleaned gas is then reheated to the process temperature before the following upgrading steps. This cooling and reheating cycle implies significant loss of energy in the process. The ability to clean the produced gas at the gasifier exit temperature would help minimize the loss of chemical energy and safeguard the downstream catalytic process units.

The performance of a cleaning device depends mainly on the particle size distribution present at the operating temperature. Also the chemical composition and volatility of the particulate matter may influence the observed filtration efficiency when particles are detected upstream and downstream a filter. For example volatile material such as tars may pass high-temperature cleaning devices in the gas-phase and condense or nucleate into particles at lower temperatures downstream the cleaning system. Therefore, it is crucial to investigate mechanisms of fine particle formation in thermochemical conversion of biomass and also to fully characterize the particulate matter present in the product gas.

Particle sampling at high temperatures almost always gives rise to some artifacts due to particle formation and transformation during the sampling process. Particle dynamics during sampling and dilution are highly non-linear and small changes in dilution and sampling conditions may result in formation of large quantities of particles in terms of both mass and number. Jimenez et. al. (2005) studied different methods for sampling of high temperature combustion aerosols [18]. They found that a quenching probe, based on aerodynamic quenching, can be advantageous at high temperatures due to the capacity to separate the particles that are formed during the sampling from the particles present at the higher temperature. Because of the very fast cooling rate (~10^8 K/s) in the quenching probe the volatile material, present in gas phase, always nucleated into very small particles. Deuerling et al. (2009) have successfully demonstrated a sampling system consisting of a porous tube dilutor and used it to analyze high temperature combustion aerosols [19]. They found that this type of dilution system can be suitable to minimize losses and artifacts of condensation and coagulation. However, one of the main problems with particle sampling from gasifiers is the vast presence of tar compounds that would dominate the obtained particle concentration when using such probe. The sampling system used in this study consists of a dilution probe, followed by a denuder with which volatile compounds can be adsorbed during cool down and therefore preventing the material to contribute to the particle phase at lower temperatures. The system has been evaluated at lab-scale where model aerosols were produced. The model aerosols consisted of either solid spherical KCl particles or agglomerated soot particles internally mixed with dioctylsebacete (DOS). The laboratory evaluations were performed at 200 °C. At this temperature the DOS will be in gas phase, while the KCl and soot remains in the particle phase. The efficiency of the dilution setup to prevent the DOS from contributing to the particle phase during cool down for subsequent characterization is presented.

2. Experimental section

2.1 Particle sampling system

The designed particle sampling setup is depicted in Fig. 1 and a cross section of the dilution probe is shown in Figure 2. The dilution probe consisted of an inner tube (i.d. 8mm) centered in a larger tube (i.d. 12mm). The dilution took place at the tip of the inner tube where the dilution air was mixed with the sample. A heating tape was used to heat up the entire probe and the dilution air to the same temperature. During measurements the probe was heated to 200 ^{o}C, which was the temperature of the sampled aerosol. Although 200 ^{o}C was chosen as the sampling temperature (due to the chosen model compounds) the heating tape and the construction material of the probe (Inconel 600) makes it possible to apply temperatures as high as 900 ^{o}C. Downstream the probe the diluted sample was split into two lines. A majority of the flow was discarded but a smaller portion (0.3-3 lpm) was drawn through a denuder where a temperature decrease, from 200 ^{o}C towards ambient temperature (20 ^{o}C) occurred. The dilution flow rate in the probe ranged from 3 to10 lpm and the sampling flow rate ranged from 0.15 to 0.30 lpm.

The denuder, shown in Figure 2, consisted of an outer stainless steel tube and an inner steel net, shaped like a tube. The inner net-tube (i.d. 10 mm) was centered in the outer tube (i.d. 31 mm) with the annular space between them filled with activated charcoal (Norit RB4). As the diffusivity is much higher for gas molecules, compared to solid or liquid particles, the concept is to adsorb the organics on the activate carbon in the denuder before the volatile material will condense on the existing particles. The design of the denuder, with a center pathway, is meant to minimize the particle losses in the diluted stream. A pre-requisite to take full advantage of the denuder is therefore to keep the flow laminar and avoid turbulence.

The total length of the heated probe was 800 mm. The main intention of having a probe of this length was that it makes it possible to use the probe in a way were it can be inserted into a gasifier product stream and to use the hot product gas, instead of a heating tape, to heat up the probe. For soot measurements a shorter probe, with a length of 350 mm, was used. The temperature profile in the probe was kept the same and the decreased residence time in the shorter probe is not believed to affect the particles characteristics. The total particle losses in the sampling system has been studied previously [20].

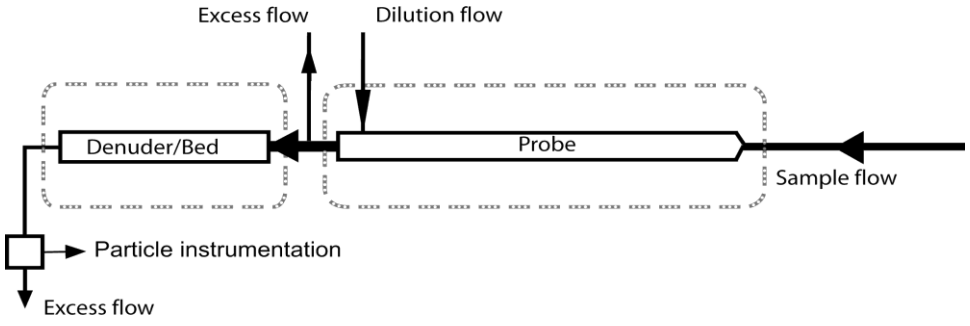

Figure 1. Experimental setup for overall particle generation, sampling and characterization

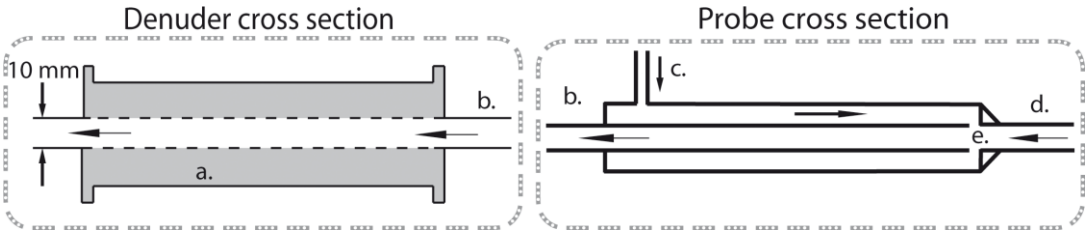

Figure 2. Design of denuder filled with adsorbent, and heated dilution probe. a) activated carbon b) diluted sample c) dilution flow d) sample flow e) dilution point

2.2 Aerosol particle characterization techniques

A Scanning Mobility Particle Sizer system (SMPS) consisting of a differential mobility analyzer (Long column DMA, TSI Inc.) and a condensation particle counter (CPC 3022, TSI Inc.) was used to determine the number size distribution of particles with electrical mobility diameters (d_m) ranging from 14 to 764 nm.

The SMPS measures the mobility equivalent diameter of the particles and spheres are assumed when the particle mass is determined. The SMPS is therefore not a sufficient characterization technique when doing quantitative mass studies of complex agglomerates like soot [20]. However, using a complementary set-up with an Aerosol Particle Mass Analyzer (APM) the mass of soot particles, and the fraction of condensed material, can be accurately measured. The APM is an online instrument with a detection limit of about 10 ag with a precision of about 5%. It consists of an outer (r_2) and an inner (r_1) cylinder rotating at the same angular speed ω. The aerosol is introduced in the gap between the cylinders and a voltage (V_{APM}) is applied to the inner cylinder while keeping the outer cylinder grounded. Thus, the force keeping the charged particles in orbit is the electrical force, balanced by the centrifugal force. Since the centrifugal force is mass dependent, the particle mass can be determined according to:

$$m = \frac{qE}{r\,\omega^2} = \frac{qV_{APM}}{r^2\omega^2 \ln\left(r_2 / r_1\right)} \qquad (1)$$

where r is the average radial distance to the gap between the cylinders from the axis of rotation ((r_2 - r_1)/2), q the particle charge and E the electrical field. The APM is described in more detail elsewhere [21].

In this study the APM (model 3600, Kanomax) was coupled in series downstream a DMA (Long column, TSI Inc.) and upstream a CPC (model 3010, TSI Inc.) This meant that the measured mass could be related to a specific mobility diameter and the particle effective densities and mass-mobility relationship could be determined [21]. The DMA was operated at a sheath flow rate of 6 lpm and an aerosol flow rate of 1 lpm. The mass distribution of particles of a selected mobility size is determined by stepping the APM voltage within a certain range depending on the particle mass and the APM rotational speed. As shown in Figure 4, a heater was introduced between DMA and APM. This heater could be by-passed and by comparing the particle mass with and without heater the amount of condensed organics on the soot particles could be determined.

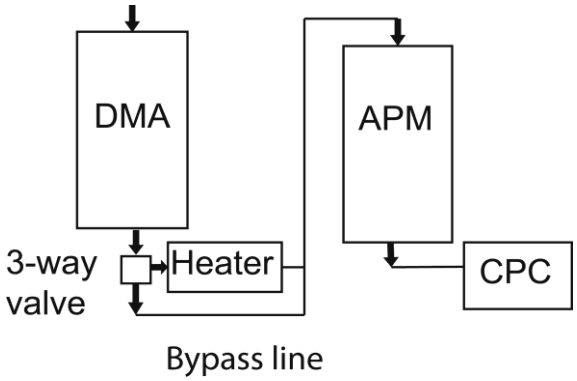

Figure 4: DMA-Heater-APM setup for evaluation of organic fraction present in soot particles coated with DOS.

The heater consisted of a 400 mm long, 31 mm inner diameter stainless steel pipe, heated to 275 °C. Because the heater was located after the DMA the total particle concentrations was low and any recondensation would occur on the tube walls instead of on the non-volatile particles. Pagels et al. [22] have shown that condensed material can be removed with a similar heater with recondensation onto the particles being less than 2%.

2.3 Generation of model compounds

The generation of KCl particles was achieved with a nebulizer in which the particle mass concentration and size distribution generated is dependent on the applied pressure and the concentration of the salt solution. The solution concentration was 200 mg/m^3. In complementary experiments, soot instead of KCl, was used as non-volatile cores. This was done to highlight the importance of selecting appropriate analytical techniques dependent on the characteristics of the agglomerated morphology of the soot particles. When using soot as model particles, the aerosol particle generation system was modified. The nebulizer was replaced by a co-flow diffusion flame soot generator, and an ejector diluter was installed upstream of the tar condensation generation system. Further description of the soot generator can be found elsewhere [23].

The concentrations of tars present in real gasifier product gas are significant and in order to mimic the presence of both solid and condensable material DOS ($C_{26}H_{50}O_4$, M_w=426 gmol^{-1}, Boiling point 212 ^oC) was introduced as a tar model compound. The vapour pressure of the DOS is sufficiently low for the DOS to be exclusively present in particle phase at room temperature. DOS has also been chosen as model compound in other investigations [6-7, 9]. The generated solid particle cores were coated with DOS in a condensation aerosol generation system (model SLG 270, TOPAS Germany), presented in Figure 2. This instrument is based on the evaporation-condensation principle and gives the means to generate internally mixed particles of controlled composition and size. The obtained mass fraction of DOS condensed on the solid particles was controlled by adjusting the flow rate through the saturator and the saturator temperature. A higher flow rate through the saturator resulted in a higher amount of solid core surface for the DOS to condense on. This flow rate therefore affected the final particle size distribution exiting the aerosol generation system. To ensure that the volatile material was condensed on the existing solid particles, and that no new particles were formed through nucleation of

evaporated organics, the aerosols were passed through a re-heater where the organics were evaporated and re-condensed on the particles.

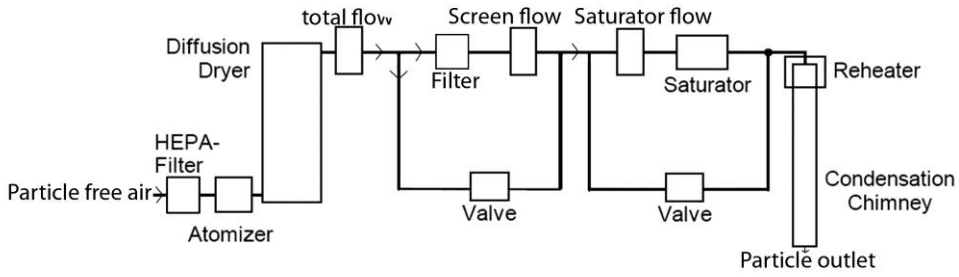

Figure 2. Condensation aerosol generation system (model SLG270, TOPAS Inc.) reproduced from [24].

The aerosol model compounds exiting the generation system, containing both DOS and KCl (or soot) were heated to 200 °C to simulate conditions in the gasification system, where the condensable matter (DOS) would be in the gas phase. The real particle size distribution and characteristics at this temperature is therefore that of KCl, as it exists before condensation of the tars. The primary aim with the measurements was to design a system which was able to extract and analyze these particles without the influence of the condensed organic fraction. To do this, and because the on-line particle characterization takes place at room temperature, the organic fraction needs to be removed from the system before the temperature reaches below the condensation point of the tars The probe, heated to 200 °C, was used to draw a sample from the generated aerosol and diluted the sample stream with particle free air. The dilution ratio ranged from 1:10 to 1:100 for KCl and was 1:10 for the soot test cases. The mass of organics on the KCl is obtained from the SMPS volume calculation where spherical particles with known density for KCl (ρ_{KCl} = 1.98 g/cm^3) and DOS oil (ρ_{DOS} = 0.915 g/cm^3) are assumed.

2.4 Generated particles with volatile organic fraction condensed on solid cores

In table 1 the characteristics of the internally mixed KCl-DOS and soot-DOS particles are given, where the total mass concentration has been calculated based on volume measurement of KCl by SMPS and density corrected mass of soot by APM. In each case of KCl and soot, the particles were coated with different amounts of DOS to investigate the removal capacity of the designed methodology. During case 1, for both KCl and soot, measurements were performed without actively introducing any DOS to the particles. However the tubes in the generation system always contained some amount of DOS, which meant that some degree of condensation on the solid KCl and soot cores were unavoidable.

Table 1: Generated model compounds of non volatile core KCl and soot loaded with DOS as volatile fraction

Test cases	DOS	Mass Median Diameter (nm)	Solid nuclei mass conc. (mg/m^3)[a]	Total mass conc. (mg/m^3)
		KCl case		
KCl-1	low	104	0.49	1.3
KCl-2	Medium	278	0.49	23
KCl-3	High	408	0.49	52
		Soot case		
Soot-1	Low	126	0.36	0.5
Soot-2	Medium	475	0.39	65
Soot-3	High	550	0.52	122
Soot-4	Very high	645	0.49	158

[a] Soot mass concentrations are corrected for average effective densities obtained by APM.

3. Results and discussion

3.1 Adsorption capacity of the denuder at different DOS inlet concentrations

The capacity of the denuder as a function of DOS inlet concentration was studied by using different dilution ratios in the probe and by varying the amount of undiluted DOS. The flow rate through the denuder was set to 0.3 lpm. Four different dilution ratios (10x, 30x, 50x and 100x) and three different model aerosol concentrations prior to dilution (1.3, 23 and 52 mg/m^3) were used. The effect on the obtained size distribution is most evident when using the KCl-3 case, which is related to the highest starting concentration of DOS. The number size distributions for this case are shown in Figure 5.

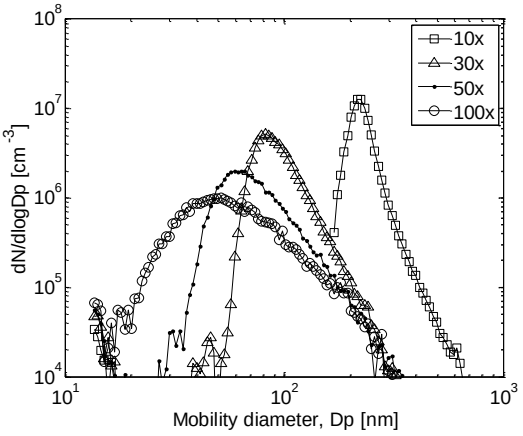

Figure 5: Number size distribution of case KCl-3 (52 mg/m^3 prior to dilution) obtained after probe-denuder with different dilution ratios at 200 °C (denuder flow rate of 0.3 lpm).

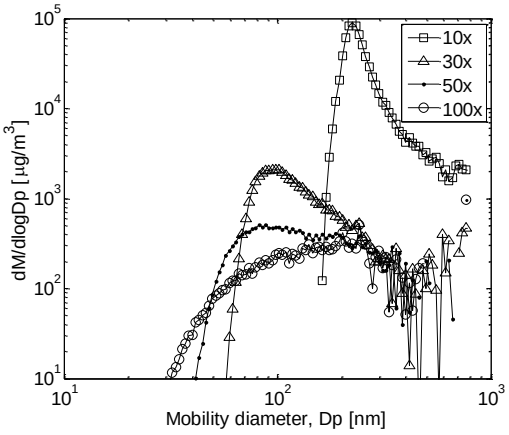

Figure 6: Mass size distribution of the KCl-3 case obtained after probe-denuder with different dilution ratios at 200 °C (denuder flow rate of 0.3 lpm).

The results from the tests show that the number size distribution shifted towards larger particle sizes with increasing DOS concentration. The lower the dilution ratio, the more condensation of organics occurs on the existing solid KCl particles. Condensation preferentially occurs on the smaller particles due to larger surface to apparent density ratio and tend to cool more rapidly than large size particles [25]. Therefore narrowing of the distributions towards larger sizes was apparent when the DOS denuder inlet concentration was higher than about 1 mg/m^3. The geometric mean diameter (GMD) of the number size distribution changed from 55 nm to 218 nm as the dilution was reduced from 100 to 10 times. In the case of flow rate 0.3 lpm, the number size distribution was affected by dilution ratios up to 50 times.

The mass weighted size distributions in Fig. 6 also show a similar trend with significant influences for dilution ratios of 10x - 50x. One exception is that the Mass Median diameter (MMD) actually decreases, from 174 to 128 nm, as the dilution ratio is decreased from 100 to 50 times. This is again because of the preferential condensation on smaller particles.

Figure 7 shows the influence of the dilution ratio on total mass concentration for all three KCl cases. The total KCl core mass concentration was between 0.4-0.5 mg/m^3 for all cases and any mass concentration above this can be attributed to condensed organics. The results show that a dilution ratio of 10 to 30 was not enough to avoid significant contribution of the organics to the total particle mass concentration during KCl-3, nor for KCl-2. On a mass basis a dilution of 50x was found suitable to avoid essentially all condensation of organics on the KCl nuclei for all concentrations. The small difference between the cases that can be spotted at the higher dilution ratio (100 times) can partly be explained by uncertainties in determination of the dilution ratio in the probe when the sampling flow rate and the dilution flow rate differed a lot.

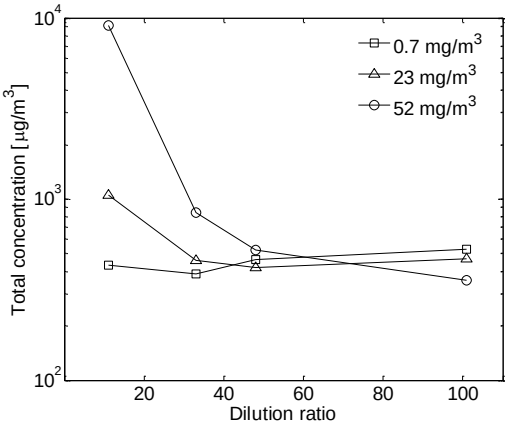

Figure 7: Dilution corrected mass concentration of KCl-DOS particles after the probe-denuder setup as a function of dilution ratio. Three different probe inlet DOS concentrations (0.7, 23, 52 mg/m^3) are presented. The mass concentration of the pure salt aerosol was about 0.4-0.5 mg/m3 for all the studied cases and the denuder flow rate was 0.3 lpm.

3.2 Effect of denuder flow rate on adsorption capacity

The capability of the denuder to adsorb the volatile component at different flow rates was tested. Figure 8 presents results from test where three different denuder flow rates, 0.3, 1 and 3 l/min, were studied using KCl as the solid core. The total KCl concentration for all cases was 0.4-0.5 mg/m^3 and dilution ratios of 10 and 50 were used in the heated probe. Once again a dilution ratio of about 50 was found optimum for all tested DOS loadings in terms of separating the condensable phase from the particle cores. It is shown that 10x was not sufficient to avoid considerable DOS condensation on the KCl at any denuder flows rates. However the total mass concentration obtained after the denuder was decreasing with an increased denuder flow rate, suggesting that condensation on KCl particles decreases with an increased denuder flow rate.

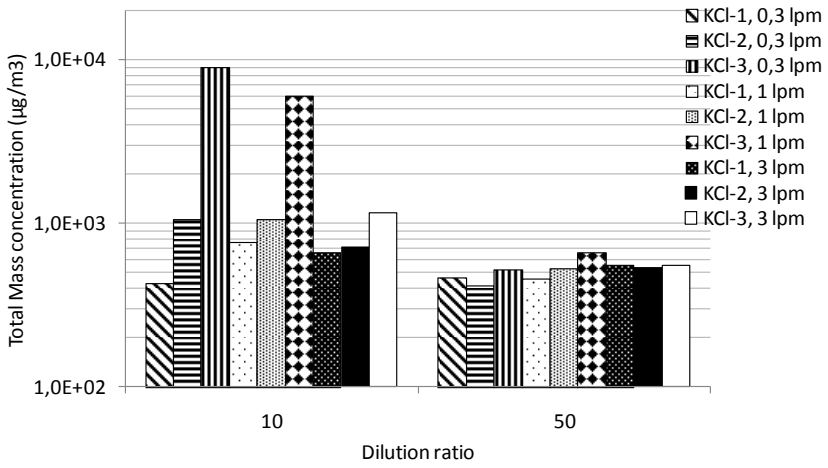

Figure 8: Total mass concentrations obtained after the denuder for different denuder flow rates and dilution ratios. The concentrations are corrected for dilution.

The DOS collection efficiency (CE) is calculated from the DOS mass concentration that goes into the denuder and the denuder outlet concentration:

$$CE\ \% = \frac{DOS\ entering\ denuder - DOS\ leaving\ the\ denuder}{DOS\ entering\ the\ denuder} \quad (2)$$

The DOS mass concentration before the probe is determined with SMPS using a density of 0.915 g/cm^3. The density-corrected mass concentration of pure KCl ($m_{KCl} = V_{KCl}\rho_{KCl}$ = 0.49 mg/m^3) is then used as a base to calculate the mass concentration of DOS after the denuder, $m_{DOS,\ after}$, as follows:

$$m_{DOS,after} = (V_{tot} - V_{KCl})\rho_{DOS} + V_{KCl}\rho_{KCl} \quad (3)$$

where V_{tot} is the total volume concentration determined by SMPS (using a density of 1 g/cm^3). The mass concentration of KCl is assumed to be the same for all cases.

The collection efficiency achieved at different denuder flow rates was calculated and is presented in Figure 9. It should be noted that the three different model aerosols presented in this figure, for 1 lpm and 3 lpm, contained slightly higher amounts of DOS than those presented in Table 1. This applies especially for the case corresponding to the highest DOS load were the DOS concentration into the denuder was 5.2-6.2 mg/m^3.

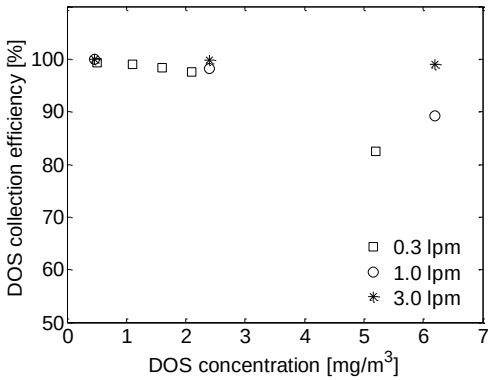

Figure 9. Collection efficiency of the denuder as a function of the inlet concentration of DOS using different denuder flow rates.

The collection efficiency was found to be >99.0 % when the denuder inlet DOS concentration was below 1 mg/m^3 for all flow rates. At 2 mg/m^3 the total collection efficiency was still high for 0.3 lpm, 97.6 %, but the small fraction that did condense on the KCl particles was, as shown in Fig. 5, enough to affect the size distribution of the KCl particles and the total particle mass concentration. When using a denuder flow rate of 3 lpm the collection efficiency was 99.0%, even for the highest DOS load.

The collection efficiencies at different denuder flow rates indicate the need to dilute the sample to a sufficient level in order to avoid significant condensation onto the existing solid particles. The lower total particle losses in the denuder, for instance compared to a bed of activated carbon come with the cost of lower collection efficiency. In the event of very high loads of condensable material, where high enough dilution ratios cannot be achieved, a packed bed of activated carbon could be advantages. Such device is reported elsewhere [20]

Since there was no active heating on the connectors between the probe and the denuder, the flow rate affected the denuder temperature profile. A higher flow rate leads to a slightly higher temperature at the entry point of the denuder. This appears to improve the adsorption capacity of the denuder. Malik et al. [20] found a collection efficiency exceeding 99.5% up to 15 mg/m3 of DOS at a flow rate of 1 lpm when active heating was used 5 cm into the denuder. Thus, the lower collection efficiency detected in our study, particularly at lower flow rates, is most likely caused by condensation of DOS in the connecting lines between the probe and the denuder. An increased flow rate also enhances the radial temperature gradient inside the denuder, which enhances the transport of gaseous compounds to the activated carbon were it can be adsorbed.

3.3 Effect of particle morphology on particle mobility diameter growth upon condensation of organics

Agglomerated particles, such as soot, contain voids in which condensation can occur without increasing the mobility size of the particle [22]. This is depicted in Fig. 10, where similar increases in the mass-ratio of organics to the particle core led to completely different influences on the particle size distributions for agglomerated soot compared to near spherical KCl. The mass ratios for soot were determined with the DMA-heater-APM technique. Even if the fraction of DOS on the solid soot particles is increased (increased m_{tot}/m_{soot} ratio) only very limited growth in mobility size is observed. The GMD of the depicted distributions in Fig. 10 only increased from 82 to 90 nm. The KCl distribution however was, as described above and shown in Fig. 10 for reference, significantly affected by condensation resulting in a narrowing distribution and an increase in number weighted geometric mean diameter from 55 nm to 87 nm. This fact is important when performing submicrometer particle measurements in environments containing irregular shaped particles and condensable material. The sampling conditions may not affect the particle mobility size even though the total mass may be increased. Sampling conditions that favor the formation of new particles through nucleation, and therefore lead to an increased number concentration, are lower temperature, lower dilution ratio and higher concentration of volatile material present in the sampled stream. To have a good estimate of the concentration of condensable material and the temperature of the stream, were sampling is to be performed, is therefore crucial in order to be able to choose a sufficient dilution ratio to avoid condensation. Further, the important factor that determines the efficiency of high temperature filters to remove nano sized particles (< 200 nm) is often particle mobility size rather than the particle mass.

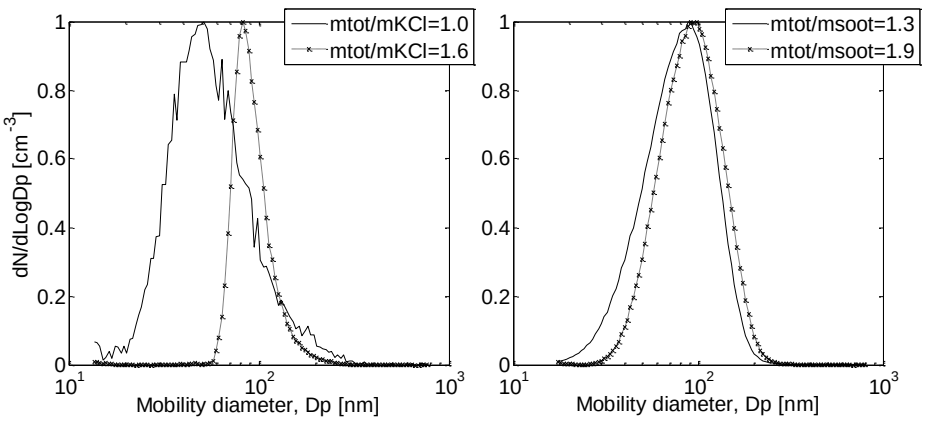

Figure 10. Effect of particle morphology on the evolution of the particle size distributions (normalized to a peak-height of 1) during condensation of DOS. Essentially no change in geometric mean diameter of the soot particles occurred during initial condensation of volatile material. m_{tot} is the total particle mass, m_{KCl} is the mass of KCl and m_{soot} is the mass of soot.

To investigate the observed effects further, simple calculations on the relationship between particle mass, effective density and mobility size for the different particle morphologies were performed. The mass, *m*, of a particle with the mobility diameter, d_{me}, can be calculated by:

$$m = \frac{\rho_{eff}\pi d_{me}^3}{6} \quad (4)$$

Where ρ_{eff} is the effective density of the particle of size d_{me}. Equation 4 can be applied for particles of any coating thickness and morphology. To predict the growth ratio, in terms of mobility diameter for spherical particles, as a function of the relative mass increase eq. 4 can be rewritten by dividing the mass of coated particles with the mass of the core particles, m_{e0}, leading to:

$$\frac{d_{me}}{d_{me0}} = \frac{m\rho_{eff0}}{m_0\rho_{eff}} \quad (5)$$

For KCl it can be assumed that the particles are spherical, or at least cube like, even without any condensation and SMPS data can be used to determine the growth ratio. In this case ρ_{eff} is equal to the inherent material density, $\rho_{true,\ mixed}$, of a spherical particle containing both a solid core and condensed material as:

$$\rho_{true,mixed} = \frac{1}{\frac{f_{DOS}}{\rho_{DOS}} + \frac{f_{nuclei}}{\rho_{nuclei}}} \quad (6)$$

Where f_{DOS} is the mass fraction of DOS on the particles and f_{nuclei} is the mass fraction of KCl or soot. ρ_{eff0} and d_{me0} is the effective density and the mean diameter of the pure solid nuclei. The calculated effective densities of the KCl + DOS particles, sampled after the denuder at different m_{tot}/m_{KCl} obtained from the experiments, follows the theoretical line of the bulk density (2 g/cm^3 for KCl and 0.915 g/cm^3 for DOS) in Fig. 11, indicating perfect spheres.

The growth ratio for aggregated soot particles undergoing condensation can be determined by using the effective densities, obtained with DMA (d_{me}) and APM (m), as a function of the mass ratio. Since the degree of agglomeration is different for different particle sizes the densities has to be determined for one mobility size at a time. Two soot particle sizes, 87 nm and 150 nm, were selected and studied with the DMA-APM setup. The 150 nm particles were close to the MMD and gave a good estimate for the average density covering the whole size distribution. The 87 nm particles were chosen to study how much higher the condensation could be on smaller particles.

The soot particles were highly agglomerated as shown by the effective densities of these particles being substantially lower than the bulk density of soot, estimated to 1.8 g/cm^3 [26]. The more material that condenses on the aggregated soot particles, the closer to a spherical shape the particle will become. This is evident in Fig. 11 as the effective density of the particles approaches that of the inherent material density of the sphere with the same composition as the mass ratio increases upon condensation.

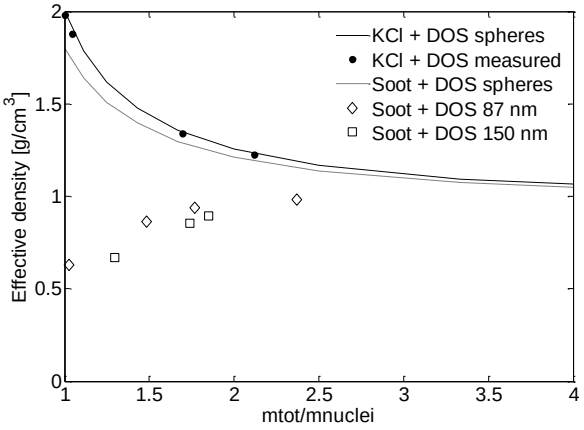

Figure 11. Bulk densities and experimental determined particle densities for KCl + DOS and soot + DOS particles. m_{tot}/m_{soot} is the ratio between total particle mass and the mass of the solid nuclei.

Using the effective densities of compact KCl and aggregated soot as a function of the mass growth factor, the mobility diameter growth factor of the particles due to condensation was estimated using eq. 5. This is shown in Figure 12. A large influence of particle morphology on the relationship between mobility diameter growth factor and mass growth factor can be seen. The calculated diametric growth factors for KCl are smaller than the ones observed from the size distributions in Fig. 10 (1.55 at m_{tot}/m_{nuclei}=1.6), while those for soot are similar to the experimentally observed factors. Qualitatively our simple model can explain the results. The most likely explanation for the discrepancy is that the organics preferentially condenses on the smaller particles in the size distribution. In the model, used in this study, average KCl masses have been used to calculate the average m_{tot}/m_{KCl}. Since the diametric growth factor during condensation increases with decreasing mobility diameter this leads to an underestimation in the simplified calculations.

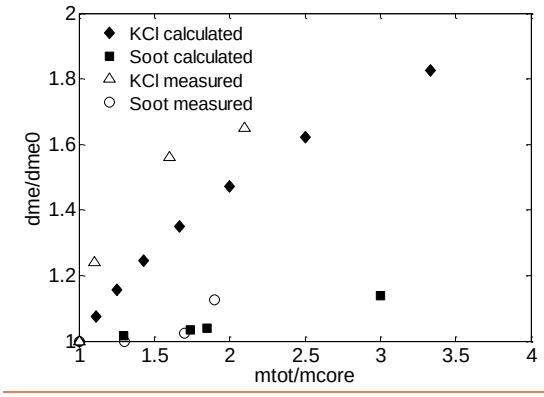

Figure 12. Calculated and measured growth rate of particle diameter as a function of the amount of condensed material. The actual rates are determined by GMD from SMPS data. The calculated value for soot is based on 150 nm particles. m_{tot}/m_{soot} is the ratio between total particle mass and the mass of the solid nuclei.

Our results clearly illustrate that agglomerated soot particles approaches a spherical shape as more and more organics condenses onto the particle in the sampling system. A similar effect is also expected for non-spherical particles undergoing condensation of low vapor pressure tars in the gasifier product gas. The results for DOS + soot are different from those found by Pagels et al. (2009) [22] where condensation of sulphuric acid on soot caused a significant decrease in the mobility diameter upon initial condensation. Thus restructuring of the soot core is substantially weaker for the soot + DOS system compared to the soot + sulphuric acid system studied by Pagels et al. (2009).

During this study relatively low concentrations of solid cores, on which condensation can occur, have been used. A lower concentration suppresses condensation on the solid cores since the available surface area for the volatile material to condense on is decreased. The use of higher concentrations might lead to lower efficiencies for the denuder which could, for instance, give significant impact on the analyzed particle size when studying compact particles. This effect on the denuder efficiency depending on the non-volatile particle concentration will need further investigation.

4. Conclusions

In this study a high temperature dilution setup was evaluated at lab-scale with different model compounds. The evaluation showed that the setup was able to avoid condensation of DOS on the existing solid particles at higher dilution ratios. The DOS collection efficiency was above 99% as long as the denuder inlet concentration was held below 1 – 6 mg/m^3, depending on the denuder flow rate. The maximum permissible DOS concentration increased with increased flow rate which can be attributed to a more favorable temperature profile at enhanced flow rates.

Evaluations with both soot and KCl as model compounds showed the effect of condensation on particles with different morphology. Compact particles such as KCl will have a much higher diameter growth factor when

subjected to condensation compared to agglomerates such as soot. This fact is important when to determine filtration efficiencies for filters to remove sub-micron particles. Total particle masses can be increased without influencing the particle size significantly.

5. Acknowledgment

The authors would like to acknowledge the financial support by the Swedish Energy Agency (STEM), the Swedish Research Council (FORMAS) and the European Commission (EC) 7th Framework Programme (GREENSYNGAS Project, Contract number 213628).

6. References

1. Strand M et al (2002) Fly ash penetration through electrostatic precipitator and flue gas condenser in a 6 MW biomass fired boiler. Energy & Fuels **16**(6):1499-1506
2. Strand M, Sanati M (2007) Fly ash elementary composition in a moving grate boiler fired with sulphur-doped woody fuel. In: Proceedings of the 15th European Biomass Conference & Exhibitio, Berlin, Germany, 7-11 May 2007
3. Pagels J et al (2003) Characteristics of aerosol particles formed during grate combustion of moist forest residue. Journal of Aerosol Science **34**(8):1043-1059
4. Carpenter DL, Deutch SP, French RJ (2007) Quantitative measurement of Biomass gasifier tars using a molecular-beam mass spectrometer: Comparison with traditional impinger sampling. Energy & Fuels **21**(5):3036-3043
5. Gustafsson E, Strand M, Sanati M (2007) Physical and chemical characterization of aerosol particles formed during the thermochemical conversion of wood pellets using a bubbling fluidized bed gasifier. Energy & Fuels **21**(6):3660-3667
6. Lindskog M, Malik A, Pagels J, Rissler J, Wierzbicka A, Sanati M (2009) Lab-Scale Development of a High Temperature Aerosol Particle Sampling Probe System. In: Proceedings of the Nordic Aerosol Conference, Lund, Sweden, 12-13 Novmber 2009
7. Lindskog M, Malik A, Pagels J, Sanati M (2010) Lab-Scale Development of a High Temperature Aerosol Particle Sampling Probe for Field Measurements in Thermochemical Conversion of Biomass. In: Proceedings of The Fifth International Conference on Thermal Engineering Theory and Applications, Marrakesh, Morocco, 10-14 May 2010
8. Gustafsson E, Strand M, Sanati M (2007) Measurement of Aerosol Particles from Steam and Oxygen Blown Gasification of Wood Pellets in a 20 kW Atmospheric Bubbling Fluidised Bed (ABFB) Gasifier. In: Proceedings of the 15th European Biomass Conference & Exhibition, ICC Berlin, Germany, 7-11 May 2007
9. Gustafsson E, Strand M (2010) Method for High-Temperature Particle Sampling in Tar-Rich Gases from the Thermochemical Conversion of Biomass. Energy & Fuels **24**:2042-2051

10. Albertazzi S, Basile F, Brandin J, Einvall J, Fornasari G, Hulteberg C, Sanati M, Trifirò F, Vaccari A (2007) Effects of fly ashes on Pt-Rh/MgAl(O) catalyst for the upgrading of the product gas from biomass gasification. In: Proceedings of the 15th European Biomass Conference & Exhibition, Berlin, Germany, 7-11 May 2007
11. Einvall J, Albertazzi S, Hulteberg C, Basile F, Larsson A-C, Gustafsson E, Brandin J, Trifirò F, Sanati M (2006) In: Proceedings of the Nordic Catalyst Society, Trondheim, Norway
12. Sanati, M et al (2007) Investigation of reforming catalyst deactivation by exposure to fly ash from biomass gasification in laboratory scale. Energy & Fuels **21**(5):2481-2488
13. Heidenreich S, Nacken M, Salinger M, Foscolo PU, Rapagna S (2008) In: Proceedings of the 7th International Symposium on Gas Cleaning at High Temperatures, Newcastle, Australia, 23-25 June 2008
14. Rapagna S et al (2009) In Situ Catalytic Ceramic Candle Filtration for Tar Reforming and Particulate Abatement in a Fluidized-Bed Biomass Gasifier. Energy & Fuels **23**(7):3804-3809
15. Toledo JM, Corella J, Molina G (2006) Catalytic hot gas cleaning with monoliths in biomass gasification in fluidized beds. 4. Performance of an advanced, second-generation, two-layers-based monolithic reactor. Industrial & Engineering Chemistry Research **45**(4):1389-1396
16. Diaz-Somoano M, Martinez-Tarazona AR (2005) Retention of zinc compounds in solid sorbents during hot gas cleaning processes. Energy & Fuels **19**(2):442-446
17. Delgado J, Aznar MP, Corella J (1997) Biomass gasification with steam in fluidized bed: Effectiveness of CaO, MgO, and CaO-MgO for hot raw gas cleaning. Industrial & Engineering Chemistry Research **36**(5):1535-1543
18. Jimenez S, Ballester J (2005) A comparative study of different methods for the sampling of high temperature combustion aerosols. Aerosol Science and Technology **39**(9):811-821
19. Deuerling CF et al (2010) Measurement System for Characterization of Gas and Particle Phase of High Temperature Combustion Aerosols. Aerosol Science and Technology **44**(1):1-9
20. Malik A, Nilsson PT, Pagels J, Lindskog M, Rissler J, Gudmundsson A, Bohgard M, Sanati M (2011) Methodology for Sampling and Characterizing Internally Mixed Soot-Tar Particles Suspended in the Product Gas from Biomass Gasification Processes. Accepted in Energy & Fuels
21. Ehara K, Hagwood C, Coakley KJ (1996) Novel method to classify aerosol particles according to their mass-to-charge ratio - Aerosol particle mass analyser. Journal of Aerosol Science **27**(2):217-234
22. Pagels J et al (2009) Processing of Soot by Controlled Sulphuric Acid and Water CondensationMass and Mobility Relationship. Aerosol Science and Technology **43**(7):629-640
23. Sanati M et al (2011) A Potential Soot Mass Determination Method from Resistivity Measurement of Thermophoretically Deposited Soot. Aerosol Science and Technology **45**(2):284-294
24. http://www.topas-gmbh.de/dateien/prospekt/250_270prspe.pdf.
25. Hinds WC (1999) Aerosol Technology, Properties, Behavior and Measurement of Airborne Particles. 2nd ed. New York: John wiley & Sons, Inc. NY
26. Park K et al (2004) Measurement of inherent material density of nanoparticle agglomerates. Journal of Nanoparticle Research **6**(2-3):267-272